

Cross Section and Parity Violating Spin Asymmetries of W^\pm Boson Production in Polarized $p + p$ Collisions at $\sqrt{s} = 500$ GeV

A. Adare,¹¹ S. Afanasiev,²⁵ C. Aidala,³⁴ N.N. Ajitanand,⁵⁶ Y. Akiba,^{50,51} R. Akimoto,¹⁰ J. Alexander,⁵⁶ H. Al-Taani,⁴⁴ K.R. Andrews,¹ A. Angerami,¹² K. Aoki,⁵⁰ N. Apadula,⁵⁷ E. Appelt,⁶¹ Y. Aramaki,¹⁰ R. Armendariz,⁶ E.C. Aschenauer,⁵ T.C. Awes,⁴⁶ B. Azmoun,⁵ V. Babintsev,²¹ M. Bai,⁴ B. Bannier,⁵⁷ K.N. Barish,⁶ B. Bassalleck,⁴³ A.T. Basye,¹ S. Bathe,⁵¹ V. Baublis,⁴⁹ C. Baumann,³⁹ A. Bazilevsky,⁵ R. Belmont,⁶¹ R. Bennett,⁵⁷ A. Berdnikov,⁵³ Y. Berdnikov,⁵³ D.S. Blau,³⁰ J.S. Bok,⁶³ K. Boyle,⁵¹ M.L. Brooks,³⁴ H. Buesching,⁵ V. Bumazhnov,²¹ G. Bunce,^{5,51} S. Butsyk,³⁴ S. Campbell,⁵⁷ A. Caringi,⁴⁰ C.-H. Chen,⁵⁷ C.Y. Chi,¹² M. Chiu,⁵ I.J. Choi,^{22,63} J.B. Choi,⁸ R.K. Choudhury,³ P. Christiansen,³⁶ T. Chujo,⁶⁰ O. Chvala,⁶ V. Cianciolo,⁴⁶ Z. Citron,⁵⁷ B.A. Cole,¹² Z. Conesa del Valle,³² M. Connors,⁵⁷ M. Csanád,¹⁵ T. Csörgő,²⁸ S. Dairaku,^{31,50} A. Datta,³⁸ G. David,⁵ M.K. Dayananda,¹⁸ A. Denisov,²¹ A. Deshpande,^{51,57} E.J. Desmond,⁵ K.V. Dharmawardane,⁴⁴ O. Dietzsch,⁵⁴ A. Dion,⁶⁴ M. Donadelli,⁵⁴ L. D Orazio,³⁷ O. Drapier,³² A. Drees,⁵⁷ K.A. Drees,⁴ J.M. Durham,⁵⁷ A. Durum,²¹ Y.V. Efremenko,⁴⁶ T. Engelmores,¹² A. Enokizono,⁴⁶ H. En'yo,^{50,51} S. Esumi,⁶⁰ B. Fadem,⁴⁰ D.E. Fields,⁴³ M. Finger, Jr.,⁷ M. Finger,⁷ F. Fleuret,³² S.L. Fokin,³⁰ J.E. Frantz,⁴⁵ A. Franz,⁵ A.D. Frawley,¹⁷ Y. Fukao,⁵⁰ T. Fusayasu,⁴² I. Garishvili,⁵⁸ A. Glenn,³³ M. Gonin,³² Y. Goto,^{50,51} R. Granier de Cassagnac,³² N. Grau,¹² S.V. Greene,⁶¹ M. Grosse Perdekamp,²² T. Gunji,¹⁰ L. Guo,³⁴ H.-Å. Gustafsson,^{36,*} J.S. Haggerty,⁵ K.I. Hahn,¹⁶ H. Hamagaki,¹⁰ J. Hamblen,⁵⁸ J. Hanks,¹² R. Han,⁴⁸ K. Hashimoto,^{52,50} E. Haslum,³⁶ R. Hayano,¹⁰ T.K. Hemmick,⁵⁷ T. Hester,⁶ X. He,¹⁸ J.C. Hill,⁶⁴ R.S. Hollis,⁶ W. Holzmann,¹² K. Homma,²⁰ B. Hong,²⁹ T. Horaguchi,⁶⁰ Y. Hori,¹⁰ D. Hornback,⁴⁶ S. Huang,⁶¹ T. Ichihara,^{50,51} R. Ichimiya,⁵⁰ H. Inuma,²⁷ Y. Ikeda,^{50,52,60} K. Imai,^{31,50} M. Inaba,⁶⁰ A. Iordanova,⁶ D. Isenhower,¹ M. Ishihara,⁵⁰ M. Issah,⁶¹ A. Isupov,²⁵ D. Ivanishev,⁴⁹ Y. Iwanaga,²⁰ B.V. Jacak,^{57,†} J. Jia,^{5,56} X. Jiang,³⁴ B.M. Johnson,⁵ T. Jones,¹ K.S. Joo,⁴¹ D. Jouan,⁴⁷ J. Kamin,⁵⁷ S. Kaneti,⁵⁷ B.H. Kang,¹⁹ J.H. Kang,⁶³ J. Kapustinsky,³⁴ K. Karatsu,^{31,50} M. Kasai,^{52,50} D. Kallow,^{38,51} A.V. Kazantsev,³⁰ T. Kempel,⁶⁴ A. Khanzadeev,⁴⁹ K.M. Kijima,²⁰ B.I. Kim,²⁹ D.J. Kim,²⁶ E.J. Kim,⁸ J.S. Kim,¹⁹ Y.-J. Kim,²² Y.K. Kim,¹⁹ E. Kinney,¹¹ Á. Kiss,¹⁵ E. Kistenev,⁵ D. Kleinjan,⁶ P. Kline,⁵⁷ L. Kochenda,⁴⁹ B. Komkov,⁴⁹ M. Konno,⁶⁰ J. Koster,²² D. Kotov,⁴⁹ A. Král,¹³ G.J. Kunde,³⁴ K. Kurita,^{52,50} M. Kurosawa,⁵⁰ Y. Kwon,⁶³ G.S. Kyle,⁴⁴ R. Lacey,⁵⁶ Y.S. Lai,¹² J.G. Lajoie,⁶⁴ A. Lebedev,⁶⁴ D.M. Lee,³⁴ J. Lee,¹⁶ K.B. Lee,²⁹ K.S. Lee,²⁹ S.R. Lee,⁸ M.J. Leitch,³⁴ M.A.L. Leite,⁵⁴ P. Lichtenwalner,⁴⁰ S.H. Lim,⁶³ L.A. Linden Levy,¹¹ A. Litvinenko,²⁵ H. Liu,³⁴ M.X. Liu,³⁴ X. Li,⁹ B. Love,⁶¹ D. Lynch,⁵ C.F. Maguire,⁶¹ Y.I. Makdisi,⁴ A. Malakhov,²⁵ V.I. Manko,³⁰ E. Mannel,¹² Y. Mao,^{48,50} H. Masui,⁶⁰ M. McCumber,⁵⁷ P.L. McGaughey,³⁴ D. McGlinchey,¹⁷ C. McKinney,²² N. Means,⁵⁷ M. Mendoza,⁶ B. Meredith,²² Y. Miake,⁶⁰ T. Mibe,²⁷ A.C. Mignerey,³⁷ K. Miki,⁶⁰ A. Milov,⁶² J.T. Mitchell,⁵ Y. Miyachi,^{50,59} A.K. Mohanty,³ H.J. Moon,⁴¹ Y. Morino,¹⁰ A. Morreale,⁶ D.P. Morrison,⁵ T.V. Moukhanova,³⁰ T. Murakami,³¹ J. Murata,^{52,50} S. Nagamiya,²⁷ J.L. Nagle,¹¹ M. Naglis,⁶² M.I. Nagy,²⁸ I. Nakagawa,^{50,51} Y. Nakamiya,²⁰ K.R. Nakamura,^{31,50} T. Nakamura,⁵⁰ K. Nakano,⁵⁰ J. Newby,³³ M. Nguyen,⁵⁷ M. Nihashi,²⁰ R. Nouicer,⁵ A.S. Nyanin,³⁰ C. Oakley,¹⁸ E. O'Brien,⁵ C.A. Ogilvie,⁶⁴ K. Okada,⁵¹ M. Oka,⁶⁰ A. Oskarsson,³⁶ M. Ouchida,²⁰ K. Ozawa,¹⁰ R. Pak,⁵ V. Pantuev,⁵⁷ V. Papavassiliou,⁴⁴ B.H. Park,¹⁹ I.H. Park,¹⁶ S.K. Park,²⁹ S.F. Pate,⁴⁴ H. Pei,⁶⁴ J.-C. Peng,²² H. Pereira,¹⁴ V. Peresedov,²⁵ D.Yu. Peressounko,³⁰ R. Petti,⁵⁷ C. Pinkenburg,⁵ R.P. Pisani,⁵ M. Proissl,⁵⁷ M.L. Purschke,⁵ H. Qu,¹⁸ J. Rak,²⁶ I. Ravinovich,⁶² K.F. Read,^{46,58} K. Reygers,³⁹ V. Riabov,⁴⁹ Y. Riabov,⁴⁹ E. Richardson,³⁷ D. Roach,⁶¹ G. Roche,³⁵ S.D. Rolnick,⁶ M. Rosati,⁶⁴ S.S.E. Rosendahl,³⁶ P. Rukoyatkin,²⁵ B. Sahlmueller,³⁹ N. Saito,²⁷ T. Sakaguchi,⁵ V. Samsonov,⁴⁹ S. Sano,¹⁰ M. Sarsour,¹⁸ T. Sato,⁶⁰ M. Savastio,⁵⁷ S. Sawada,²⁷ K. Sedgwick,⁶ R. Seidl,⁵¹ R. Seto,⁶ D. Sharma,⁶² I. Shein,²¹ T.-A. Shibata,^{50,59} K. Shigaki,²⁰ H.H. Shim,²⁹ M. Shimomura,⁶⁰ K. Shoji,^{31,50} P. Shukla,³ A. Sickles,⁵ C.L. Silva,⁶⁴ D. Silvermyr,⁴⁶ C. Silvestre,¹⁴ K.S. Sim,²⁹ B.K. Singh,² C.P. Singh,² V. Singh,² M. Slunečka,⁷ R.A. Soltz,³³ W.E. Sondheim,³⁴ S.P. Sorensen,⁵⁸ I.V. Sourikova,⁵ P.W. Stankus,⁴⁶ E. Stenlund,³⁶ S.P. Stoll,⁵ T. Sugitate,²⁰ A. Sukhanov,⁵ J. Sun,⁵⁷ J. Sziklai,²⁸ E.M. Takagui,⁵⁴ A. Takahara,¹⁰ A. Taketani,^{50,51} R. Tanabe,⁶⁰ Y. Tanaka,⁴² S. Taneja,⁵⁷ K. Tanida,^{31,50,51,55} M.J. Tannenbaum,⁵ S. Tarafdar,² A. Taranenko,⁵⁶ E. Tennant,⁴⁴ H. Themann,⁵⁷ D. Thomas,¹ M. Togawa,⁵¹ L. Tomášek,²³ M. Tomášek,²³ H. Torii,²⁰ R.S. Towell,¹ I. Tserruya,⁶² Y. Tsuchimoto,²⁰ K. Utsunomiya,¹⁰ C. Vale,⁵ H.W. van Hecke,³⁴ E. Vazquez-Zambrano,¹² A. Veicht,¹² J. Velkovska,⁶¹ R. Vértesi,²⁸ M. Virius,¹³ A. Vossen,²² V. Vrba,²³ E. Vznuzdaev,⁴⁹ X.R. Wang,⁴⁴ D. Watanabe,²⁰ K. Watanabe,⁶⁰ Y. Watanabe,¹⁰ Y. Watanabe,^{50,51} F. Wei,⁶⁴ J. Wessels,³⁹ S.N. White,⁵ D. Winter,¹² C.L. Woody,⁵ R.M. Wright,¹ M. Wysocki,¹¹ Y.L. Yamaguchi,¹⁰ R. Yang,²² A. Yanovich,²¹ J. Ying,¹⁸ S. Yokkaichi,^{50,51} J.S. Yoo,¹⁶

G.R. Young,⁴⁶ I. Younus,⁴³ Z. You,^{34, 48} I.E. Yushmanov,³⁰ W.A. Zajc,¹² A. Zelenski,⁴ S. Zhou,⁹ and L. Zolin²⁵

(PHENIX Collaboration)

- ¹Abilene Christian University, Abilene, Texas 79699, USA
²Department of Physics, Banaras Hindu University, Varanasi 221005, India
³Bhabha Atomic Research Centre, Bombay 400 085, India
⁴Collider-Accelerator Department, Brookhaven National Laboratory, Upton, New York 11973-5000, USA
⁵Physics Department, Brookhaven National Laboratory, Upton, New York 11973-5000, USA
⁶University of California - Riverside, Riverside, California 92521, USA
⁷Charles University, Ovocný trh 5, Praha 1, 116 36, Prague, Czech Republic
⁸Chonbuk National University, Jeonju, 561-756, Korea
⁹China Institute of Atomic Energy (CIAE), Beijing, People's Republic of China
¹⁰Center for Nuclear Study, Graduate School of Science, University of Tokyo, 7-3-1 Hongo, Bunkyo, Tokyo 113-0033, Japan
¹¹University of Colorado, Boulder, Colorado 80309, USA
¹²Columbia University, New York, New York 10027 and Nevis Laboratories, Irvington, New York 10533, USA
¹³Czech Technical University, Zikova 4, 166 36 Prague 6, Czech Republic
¹⁴Dapnia, CEA Saclay, F-91191, Gif-sur-Yvette, France
¹⁵ELTE, Eötvös Loránd University, H - 1117 Budapest, Pázmány P. s. 1/A, Hungary
¹⁶Ewha Womans University, Seoul 120-750, Korea
¹⁷Florida State University, Tallahassee, Florida 32306, USA
¹⁸Georgia State University, Atlanta, Georgia 30303, USA
¹⁹Hanyang University, Seoul 133-792, Korea
²⁰Hiroshima University, Kagamiyama, Higashi-Hiroshima 739-8526, Japan
²¹IHEP Protvino, State Research Center of Russian Federation, Institute for High Energy Physics, Protvino, 142281, Russia
²²University of Illinois at Urbana-Champaign, Urbana, Illinois 61801, USA
²³Institute of Physics, Academy of Sciences of the Czech Republic, Na Slovance 2, 182 21 Prague 8, Czech Republic
²⁴Iowa State University, Ames, Iowa 50011, USA
²⁵Joint Institute for Nuclear Research, 141980 Dubna, Moscow Region, Russia
²⁶Helsinki Institute of Physics and University of Jyväskylä, P.O.Box 35, FI-40014 Jyväskylä, Finland
²⁷KEK, High Energy Accelerator Research Organization, Tsukuba, Ibaraki 305-0801, Japan
²⁸KFKI Research Institute for Particle and Nuclear Physics of the Hungarian Academy of Sciences (MTA KFKI RMKI), H-1525 Budapest 114, POBox 49, Budapest, Hungary
²⁹Korea University, Seoul, 136-701, Korea
³⁰Russian Research Center "Kurchatov Institute", Moscow, Russia
³¹Kyoto University, Kyoto 606-8502, Japan
³²Laboratoire Leprince-Ringuet, Ecole Polytechnique, CNRS-IN2P3, Route de Saclay, F-91128, Palaiseau, France
³³Lawrence Livermore National Laboratory, Livermore, California 94550, USA
³⁴Los Alamos National Laboratory, Los Alamos, New Mexico 87545, USA
³⁵LPC, Université Blaise Pascal, CNRS-IN2P3, Clermont-Fd, 63177 Aubiere Cedex, France
³⁶Department of Physics, Lund University, Box 118, SE-221 00 Lund, Sweden
³⁷University of Maryland, College Park, Maryland 20742, USA
³⁸Department of Physics, University of Massachusetts, Amherst, Massachusetts 01003-9337, USA
³⁹Institut für Kernphysik, University of Muenster, D-48149 Muenster, Germany
⁴⁰Muhlenberg College, Allentown, Pennsylvania 18104-5586, USA
⁴¹Myongji University, Yongin, Kyonggido 449-728, Korea
⁴²Nagasaki Institute of Applied Science, Nagasaki-shi, Nagasaki 851-0193, Japan
⁴³University of New Mexico, Albuquerque, New Mexico 87131, USA
⁴⁴New Mexico State University, Las Cruces, New Mexico 88003, USA
⁴⁵Department of Physics and Astronomy, Ohio University, Athens, OH 45701, USA
⁴⁶Oak Ridge National Laboratory, Oak Ridge, Tennessee 37831, USA
⁴⁷IPN-Orsay, Université Paris Sud, CNRS-IN2P3, BP1, F-91406, Orsay, France
⁴⁸Peking University, Beijing, People's Republic of China
⁴⁹PNPI, Petersburg Nuclear Physics Institute, Gatchina, Leningrad region, 188300, Russia
⁵⁰RIKEN Nishina Center for Accelerator-Based Science, Wako, Saitama 351-0198, JAPAN
⁵¹RIKEN BNL Research Center, Brookhaven National Laboratory, Upton, New York 11973-5000, USA
⁵²Physics Department, Rikkyo University, 3-34-1 Nishi-Ikebukuro, Toshima, Tokyo 171-8501, Japan
⁵³Saint Petersburg State Polytechnic University, St. Petersburg, Russia
⁵⁴Universidade de São Paulo, Instituto de Física, Caixa Postal 66318, São Paulo CEP05315-970, Brazil
⁵⁵Seoul National University, Seoul, Korea
⁵⁶Chemistry Department, Stony Brook University, SUNY, Stony Brook, New York 11794-3400, USA
⁵⁷Department of Physics and Astronomy, Stony Brook University, SUNY, Stony Brook, New York 11794-3400, USA
⁵⁸University of Tennessee, Knoxville, Tennessee 37996, USA
⁵⁹Department of Physics, Tokyo Institute of Technology, Oh-okayama, Meguro, Tokyo 152-8551, Japan
⁶⁰Institute of Physics, University of Tsukuba, Tsukuba, Ibaraki 305, Japan

⁶¹*Vanderbilt University, Nashville, Tennessee 37235, USA*

⁶²*Weizmann Institute, Rehovot 76100, Israel*

⁶³*Yonsei University, IPAP, Seoul 120-749, Korea*

⁶⁴*Iowa State University, Ames, Iowa 50011, USA*

(Dated: September 7, 2010)

Large parity violating longitudinal single-spin asymmetries $A_L^{e^+} = -0.86_{-0.14}^{+0.30}$ and $A_L^{e^-} = 0.88_{-0.71}^{+0.12}$ are observed for inclusive high transverse momentum electrons and positrons in polarized $p + p$ collisions at a center of mass energy of $\sqrt{s} = 500$ GeV with the PHENIX detector at RHIC. These e^\pm come mainly from the decay of W^\pm and Z^0 bosons, and their asymmetries directly demonstrate parity violation in the couplings of the W^\pm to the light quarks. The observed electron and positron yields were used to estimate W^\pm boson production cross sections for the e^\pm channels of $\sigma(pp \rightarrow W^+ X) \times BR(W^+ \rightarrow e^+ \nu_e) = 144.1 \pm 21.2(\text{stat})_{-10.3}^{+3.4}(\text{syst}) \pm 15\%(norm)$ pb, and $\sigma(pp \rightarrow W^- X) \times BR(W^- \rightarrow e^- \bar{\nu}_e) = 31.7 \pm 12.1(\text{stat})_{-8.2}^{+10.1}(\text{syst}) \pm 15\%(norm)$ pb.

PACS numbers: 14.20.Dh, 25.40.Ep, 13.85.Ni, 13.88.+e

Determining the contributions of the partons to the spin of the proton is a crucial element in our understanding of QCD [1–3]. Polarized inclusive deep inelastic scattering experiments (DIS) have measured the combination of valence and sea quark, and gluon helicity distributions ($\Delta q + \Delta \bar{q}$, Δg) [3, 4]. Analysis of polarized semi-inclusive DIS experiments [5–7] have determined the individual flavor separated Δq and $\Delta \bar{q}$ by connecting final state hadrons with quark flavors using fragmentation functions. Collisions of longitudinally polarized protons at high energies allow study of Δg [4, 8, 9], and can provide complementary measurements of Δu , $\Delta \bar{u}$, Δd , $\Delta \bar{d}$ [10, 11]. In particular, the production of W^\pm couples only the left-handed quarks and right-handed antiquarks ($u_L \bar{d}_R \rightarrow W^+$ and $d_L \bar{u}_R \rightarrow W^-$), so the asymmetry of the W yield from flipping the helicity of a polarized proton is sensitive to the flavor dependence of Δq and $\Delta \bar{q}$. Production of the W occurs at a scale where higher order QCD corrections can be evaluated reliably, and it is free from uncertainties in fragmentation functions by detecting leptons from W decay [12, 13].

The first observations of W -boson production in polarized $p + p$ collisions, and direct demonstration of the parity-violating coupling of the W to the light quarks are reported here by PHENIX and in a companion paper by STAR [14] for $\sqrt{s} = 500$ GeV at the Relativistic Heavy Ion Collider. The 2009 PHENIX data are from polarized $pp \rightarrow e^\pm + X$, where the e^\pm with $p_T > 30$ GeV/ c come mainly from W and Z decays.

The PHENIX detector has been described in detail elsewhere [15]. This analysis is based on data collected with two central arm spectrometers, each covering $|\Delta\phi| < \pi/2$ in azimuth and $|\eta| < 0.35$ in pseudorapidity, which surround the central axial magnetic field. The bend angle of charged tracks is determined by drift chambers outside the magnetic field starting at a radius of 2.02 m from the beamline. The longitudinal position z of the track is measured as it exits the drift chamber in a layer of pad chambers 2.46 m from the beamline with a spatial resolution of $\sigma_z = 1.7$ mm.

The electromagnetic calorimeter, located at a radial distance of ~ 5 m from the beam line, is used to measure the energy, position, and time of flight of electrons. In this analysis, the p_T dependence of the reconstructed π^0 and η mass peaks was used to confirm the energy scale and linearity to within 2.5%. The p_T dependence of the peak widths was used to determine the energy resolution $\sigma_E/E = 8.1\%/\sqrt{E}(\text{GeV}) \oplus 5.0\%$.

A trigger with a nominal 10 GeV threshold in the electromagnetic calorimeter selected events for this analysis. This trigger was fully efficient for e^\pm with transverse momentum p_T above 12 GeV/ c . Charged tracks reconstructed in the drift chambers and the pad chambers which match the calorimeter cluster with $|\Delta\phi| < 0.01$ were used to reconstruct the z position of the event vertex. Only events with $|z| < 30$ cm that are well within the acceptance of the central arm spectrometers were analyzed. Loose cuts on the time of flight measured by the calorimeter and energy-momentum matching suppressed accidental matches and cosmic rays.

The analyzed data sample corresponds to an integrated luminosity of 8.6 pb^{-1} , which was determined from beam-beam counter coincidences and corrected for a small (6%) effect from multiple collisions per beam crossing. The beam-beam counters are two 64 channel quartz Čerenkov counters ± 1.44 m from the center of the detector and cover a pseudorapidity range of $3.1 < |\eta| < 3.9$. The cross section for coincidences within $|z| \lesssim 30$ cm was found to be 32.5 ± 3.2 mb from the van der Meer scan technique [16].

The resulting yield of positive and negative electron candidates is shown in Fig. 1 where p_T has been determined from the calorimeter cluster energy. The charge sign is determined from the bend angle, α , measured in the drift chamber, and the nominal transverse beam position. The angular resolution and stability of beam position were monitored by frequent runs with no magnetic field. The resolution σ_α was typically about 1.1 mr, to be compared to a 2.3 mr bend angle for 40 GeV/ c tracks. The variation in the average transverse beam po-

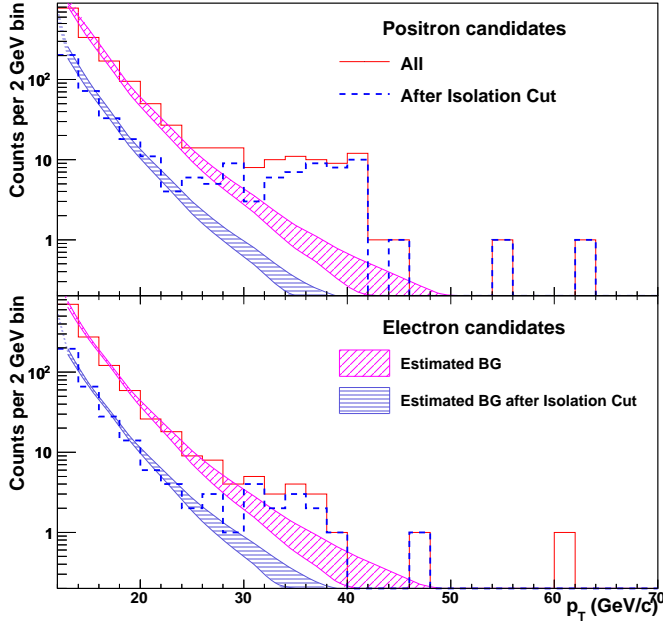


FIG. 1: (color online) The spectra of positive (upper panel) and negative (lower panel) candidates before (solid histogram) and after (dashed histogram) an isolation cut. The estimated background bands are also shown. The computation of the background before the isolation cut is described in the text. The background band after the isolation cut is computed by scaling the background before the isolation cut by the isolation cut efficiency measured in the background region ($12 < p_T < 20$ GeV/c).

sition measured by reconstruction of the primary vertex in these runs was within $\pm 300 \mu\text{m}$, and did not affect the charge determination. The probability of charge misidentification at 40 GeV/c was estimated to be less than 2%.

In addition to e^\pm from W and Z decay, this sample of events contains various backgrounds. The dominant backgrounds were photon conversions before the drift chamber and charged hadrons. These were estimated using the raw calorimeter cluster distribution and the charged pion spectra predicted by perturbative QCD convoluted with the hadronic response of the calorimeter tuned to reproduce test beam data. This calculated background was normalized to the measured spectrum in the region $12 < p_T < 20$ GeV/c and extrapolated to higher p_T . Electrons from heavy flavor decay were estimated from an FONLL calculation [17] which agrees well with the prompt electron measurement at $\sqrt{s} = 200$ GeV [18]. PYTHIA [19] was used to estimate the contributions of electrons with $p_T > 30$ GeV/c from τ lepton decays of W and Z bosons. These two components were found to be negligible. The background bands in Fig. 1 include uncertainties in the photon conversion probability, the background normalization, and the background extrapolation to $p_T > 30$ GeV/c.

The acceptance was calculated from Monte Carlo sim-

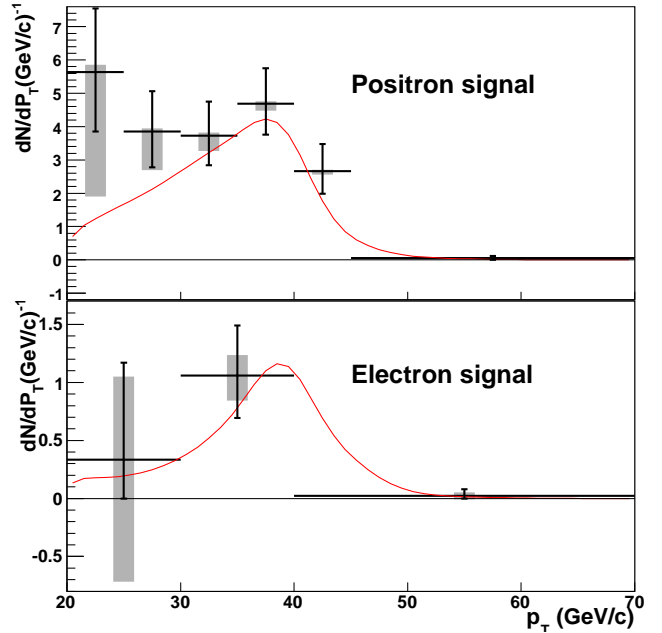


FIG. 2: (color online) Background subtracted spectra of positron (upper panel) and electron (lower panel) candidates taken from all counts compared to the spectrum of W and Z decays from an NLO calculation [12, 13] (see text). The gray bands reflect the range of background estimates.

ulation and corrected for time dependent variations in tracking and trigger efficiency measured with a minimum bias data sample triggered by beam-beam counter coincidences. The reconstruction efficiency for tracks within the geometrical acceptance of the spectrometer is the product of the active areas of the drift chamber and the pad chamber (54%), a fiducial cut on the calorimeter to ensure the showers are not near an edge (81%), and a fiducial cut on the drift chamber to avoid charge misidentification (85%). The reconstruction efficiency was not p_T dependent for $p_T > 30$ GeV/c.

Figure 2 shows the background subtracted signal in the acceptance of the detector for positive and negative charges respectively compared to the spectrum predicted by NLO calculations [12, 13, 20] normalized for the integrated luminosity, corrected for the detector efficiency and acceptance, and smeared by the energy resolution of the calorimeter. The yield measured by counting events in the signal ($30 < p_T < 50$ GeV/c) region is compared to the predicted yield in Table I. The measured yield in the signal region is consistent with the predictions of the NLO and NNLO [20] calculations.

To extract the W^\pm production cross section, we estimated the Z fraction in our sample with the NLO and NNLO calculations and MRST [21] and MSTW [22] PDFs. The contribution from Z decays is approximately $\sim 7\%$ for W^+ and $\sim 30\%$ for W^- . The fraction of the total cross section within $|y| < 0.35$, $p_T > 30$ GeV/c,

TABLE I: Comparison of measured cross sections for electrons and positrons with $30 < p_T < 50$ GeV/c from W and Z decays with NLO [12] and NNLO [20] calculations. The first error is statistical; the second error is systematic from the uncertainty in the background; the third error is a 15% normalization uncertainty due to the luminosity (10%), multiple collision (5%), and acceptance and efficiency uncertainties (10%).

Lepton	$\frac{d\sigma}{dy}(30 < p_T^e < 50 \text{ GeV}/c) _{y=0}$ [pb]		
	Data	NLO	NNLO
e^+	$50.2 \pm 7.2^{+1.2}_{-3.6} \pm 15\%$	43.2	46.8
e^-	$9.7 \pm 3.7^{+2.1}_{-2.5} \pm 15\%$	11.3	13.5
e^+ and e^-	$59.9 \pm 8.1^{+3.1}_{-6.0} \pm 15\%$	54.5	60.3

and $|\Delta\phi| < \pi$ is estimated to be $\sim 11\%$ of positrons from W^+ and $\sim 7.5\%$ of electrons from W^- from these calculations. The variation of the calculation is small compared to other sources of systematic uncertainty. With these corrections, $\sigma(pp \rightarrow W^+X) \times BR(W^+ \rightarrow e^+\nu_e) = 144.1 \pm 21.2(\text{stat})^{+3.4}_{-10.3}(\text{syst}) \pm 15\%(norm)$ pb, and $\sigma(pp \rightarrow W^-X) \times BR(W^- \rightarrow e^-\bar{\nu}_e) = 31.7 \pm 12.1(\text{stat})^{+10.1}_{-8.2}(\text{syst}) \pm 15\%(norm)$ pb, where BR is the branching ratio. These are shown in Fig. 3 and compared to published Tevatron and $Spp\bar{S}$ data.

In order to determine the longitudinal spin asymmetry with a sample of W decays with minimal background contamination, two additional requirements were imposed on the candidate events. An isolation cut requiring the sum of cluster energies in the calorimeter and transverse momenta measured in the drift chamber be less than 2 GeV in a cone with a radius in η and ϕ of 0.5 around the candidate track was used to remove remaining events with jets. About 80% of the signal is kept, while the background is reduced by a factor ~ 4 as shown in Fig. 1. The second cut is to reject tracks with $|\alpha| < 1$ mr, which reduces charge misidentification to negligible levels. There are 42 candidate $W^+ + Z^0$ decays to positrons with a background of 1.7 ± 1.0 and 13 candidate $W^- + Z^0$ decays to electrons with a background of 1.6 ± 1.0 events within $30 < p_T < 50$ GeV/c after these two additional cuts.

The measured asymmetry is given by

$$\epsilon_L = \frac{N^+ - R \cdot N^-}{N^+ + R \cdot N^-} \quad (1)$$

where N^+ is the number of events from a beam of positive helicity and N^- is the number of events from a beam of negative helicity, and R is the ratio of the luminosity for the positive and the negative helicity beams. The longitudinal spin asymmetry is then calculated from the measured asymmetry according to

$$A_L = \frac{\epsilon_L \cdot D}{P} \quad (2)$$

where P is the beam polarization and D is a dilution correction to account for the remaining background in the signal region.

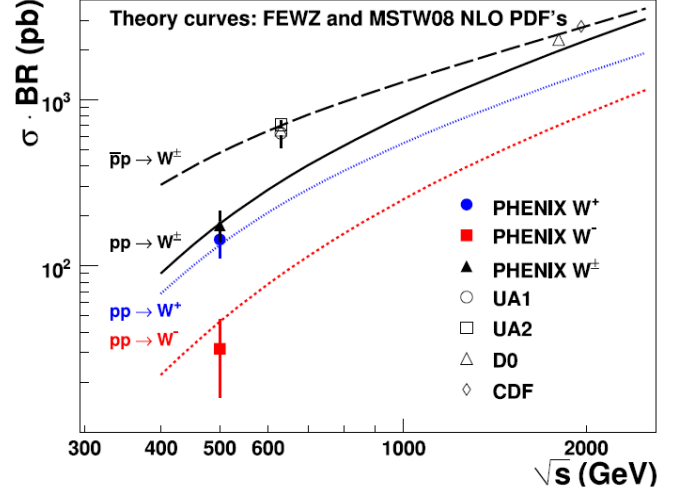


FIG. 3: (color online) Inclusive cross sections for W leptonic decay channel of this measurement and $\bar{p}p$ measurements [23–26]. Statistical and systematic uncertainties were added here in quadrature. Curves represent theory calculations.

The luminosity-weighted polarization was 0.38 ± 0.03 and 0.40 ± 0.04 in the two beams. In RHIC, both beams are bunched, and the bunch helicity alternates almost every crossing to reduce systematic effects. The relative luminosities of the four helicity combinations were measured by the beam-beam counters, and were all within 1% of each other. To treat the low statistics data properly, a likelihood function created from the four spin sorted yields corrected by the relative luminosity was used to determine the single-spin asymmetry within its physical range $[-1,1]$.

The measured asymmetries are shown in Table II for tracks in the background ($12 < p_T < 20$ GeV/c) and signal ($30 < p_T < 50$ GeV/c) regions. For tracks in the background region, ϵ_L was found to be zero within uncertainties. Significant asymmetries were observed for tracks in the signal region. The dilution corrections of 1.04 ± 0.03 and 1.14 ± 0.10 for positive and negative charges, respectively, were applied.

Figure 4 compares measured longitudinal single-spin asymmetries to estimates based on a sample of polarized PDFs extracted from fits of DIS and semi-inclusive DIS data. The experimental results are consistent with the theoretical calculations at 6-15% confidence level for $A_L^{\epsilon^+}$ and at 20-37% for $A_L^{\epsilon^-}$. The observed asymmetries are sensitive to the polarized quark densities at $x \sim M_W/\sqrt{s} \simeq 0.16$, and directly demonstrate the parity violating coupling between W bosons and light quarks.

In summary, we presented first measurements of production cross section and nonzero parity violating asymmetry in W and Z production in polarized $p+p$ collisions at $\sqrt{s} = 500$ GeV. The results are found to be consistent with theoretical expectations and similar measurements of $A_L^{\epsilon^\pm}$ [14]. RHIC luminosity and PHENIX detector

TABLE II: Longitudinal single-spin asymmetries

Sample	ϵ_L	$A_L^e(W+Z)$	68%CL	95%CL
Bkgrnd +	-0.015 ± 0.04			
Signal +	-0.31 ± 0.10	-0.86	$[-1, -0.56]$	$[-1, -0.16]$
Bkgrnd -	-0.025 ± 0.04			
Signal -	0.29 ± 0.20	+0.88	$[0.17, 1]$	$[-0.60, 1]$

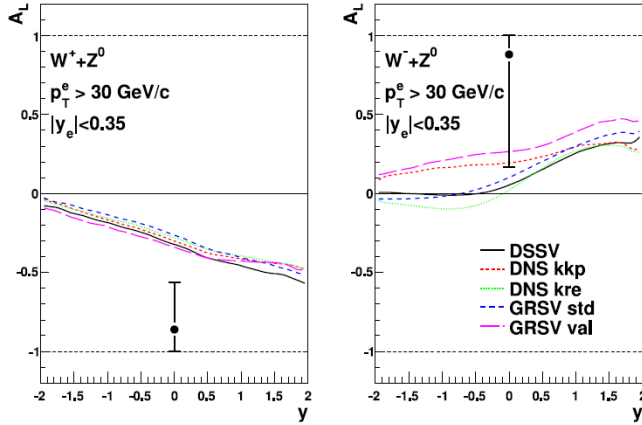


FIG. 4: (color online) Longitudinal single-spin asymmetries for electrons and positrons from W and Z decays. The error bars represent 68% CL. The theoretical curves are calculated using NLO with different polarized PDFs [12].

upgrades in progress will make it possible in the future to significantly reduce the uncertainties for A_L and to extend the measurement to forward rapidity, which will improve our knowledge of flavor separated quark and antiquark helicity distributions.

We thank the Collider-Accelerator Department for developing the unique technologies enabling these measurements and the Physics Department staff at BNL for vital contributions. We also thank D. de Florian, B. Surrow, and J. Balewski for helpful discussions. We acknowledge support from the Office of Nuclear Physics in DOE Office of Science and NSF (U.S.A.), MEXT and JSPS (Japan), CNPq and FAPESP (Brazil), NSFC (China), MSMT (Czech Republic), IN2P3/CNRS and CEA (France), BMBF, DAAD, and AvH (Germany),

OTKA (Hungary), DAE and DST (India), ISF (Israel), NRF (Korea), MES, RAS, and FAEF (Russia), VR and KAW (Sweden), U.S. CRDF for the FSU, Hungary-US HAESF, and US-Israel BSF.

* Deceased

† Spokesperson: jacak@skipper.physics.sunysb.edu

- [1] R. L. Jaffe and A. Manohar, Nucl. Phys. **B337**, 509 (1990).
- [2] E. Leader and M. Anselmino, Z. Phys. **C41**, 239 (1988).
- [3] S. E. Kuhn, J. P. Chen, and E. Leader, Prog. Part. Nucl. Phys. **63**, 1 (2009) and references therein.
- [4] D. de Florian, R. Sassot, M. Stratmann, and W. Vogelsang, Phys. Rev. **D80**, 034030 (2009).
- [5] M. G. Alekseev et al. (2010), 1007.4061.
- [6] A. Airapetian et al., Phys. Rev. **D71**, 012003 (2005).
- [7] B. Adeva et al., Phys. Lett. **B420**, 180 (1998).
- [8] A. Adare et al., Phys. Rev. Lett. **103**, 012003 (2009).
- [9] B. I. Abelev et al., Phys. Rev. Lett. **100**, 232003 (2008).
- [10] G. Bunce, N. Saito, J. Soffer, and W. Vogelsang, Ann. Rev. Nucl. Part. Sci. **50**, 525 (2000).
- [11] C. Bourrely and J. Soffer, Phys. Lett. **B314**, 132 (1993).
- [12] D. de Florian and W. Vogelsang, Phys. Rev. **D81**, 094020 (2010).
- [13] P. M. Nadolsky and C. P. Yuan, Nucl. Phys. **B666**, 31 (2003).
- [14] M. M. Aggarwal et al., arXiv:1009.0326 [hep-ex].
- [15] K. Adcox et al., Nucl. Instrum. Meth. **A499**, 469 (2003).
- [16] A. Adare et al., Phys. Rev. **D79**, 012003 (2009).
- [17] M. Cacciari, P. Nason, and R. Vogt, Phys. Rev. Lett. **95**, 122001 (2005); M. Cacciari, private communication.
- [18] A. Adare et al., Phys. Rev. Lett. **97**, 252002 (2006).
- [19] T. Sjöstrand et al., Comput. Phys. Commun. **135**, 238 (2001).
- [20] K. Melnikov and F. Petriello, Phys. Rev. **D74**, 114017 (2006).
- [21] A. D. Martin, R. G. Roberts, W. J. Stirling, and R. S. Thorne, Eur. Phys. J. **C28**, 455 (2003).
- [22] A. D. Martin, W. J. Stirling, R. S. Thorne, and G. Watt, Eur. Phys. J. **C63**, 189 (2009).
- [23] D. E. Acosta et al., Phys. Rev. Lett. **94**, 091803 (2005).
- [24] B. Abbott et al., Phys. Rev. **D61**, 072001 (2000).
- [25] J. Alitti et al., Z. Phys. **C47**, 11 (1990).
- [26] C. Albajar et al., Z. Phys. **C44**, 15 (1989).